ACS APPLIED MATERIALS & INTERFACES

Letter

www.acsami.org

Three-Dimensionally Interconnected TaS_3 Nanowire Network as Anode for High-Performance Flexible Li-Ion Battery

Weihan Li, Lei Yang, Jiaqing Wang, Bin Xiang,* and Yan Yu*

Key Laboratory of Materials for Energy Conversion, Chinese Academy of Sciences, Department of Materials Science and Engineering, University of Science and Technology of China, Hefei, Anhui 230026, P. R. China

Supporting Information

ABSTRACT: Here we demonstrated tantalum trisulfide (TaS_3) nanowires as a new self-supported and flexible anode material for Li-ion batteries with high specific capacity and excellent electrochemical cycling. The TaS_3 nanofibers were fabricated by a solid state reaction process, delivering a good reversible capacity of ~400 $mAhg^{-1}$ after 100 cycles at 0.1*C* with only 0.1% decay per cycle compared with the initial charge capacity. Cycled at 10*C*, it displays a capacity as high as 60 mAh g^{-1}. The continuous and interconnected TaS_3 nanowires not only enable fast access of electrons and ions but also grant the electrode with high mechanical flexibility.

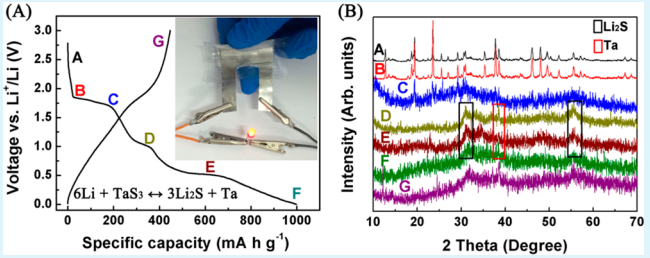

KEYWORDS: *TaS_3, lithium-storage mechanism, lithium-ion batteries, anode, flexible*

Lithium-ion batteries (LIBs) have become the main power source for wearable electronics (rollup displays, wearable devices and implantable medical devices) because of the high energy density, high output voltage, long life, and environmentally friendly operation.[1,2] To meet the requirements of high performance power sources for wearable electronics, it is necessary to fabricate flexible electrodes with high electrochemical and mechanical performance.[3,4] Some efforts have been made to explore flexible electrodes for LIBs.[4−9] Among them, introducing carbon matrix (such as graphene, carbon nanotubes, etc.) to flexible electrodes for LIBs is one of the most popular approaches for enhancing the mechanical and electrochemical performance.[10−12] However, the limited specific capacity of carbon materials could lower the specific capacity of the overall electrodes.[13] Therefore, design and development of electrode materials with a higher theoretical capacity, 3D interconnected network with a short ion diffusion path is highly beneficial for the enhanced gravimetric/volumetric performances of flexible battery.[14]

Metal sulfides have (such as α-MnS,[15] FeS_2,[16] CoS_2,[17] NiS,[18] MoS_2,[19] WS_2,[20] and CuS[21]) recently emerged as a new promising class of active materials because of their excellent reversibility and relatively high capacity. TaS_3, is an interesting conductor that has a lamellar crystal structure, whose basic crystal unit is built of S−Ta−S sandwich layers.[22] Layer-structured TaS_3 is of great potential in energy storage because their crystal structure can be easily utilized for the reversible storage of lithium.

Herein, we first report TaS_3 nanowires (NWs) with 3D interconnected structure as a new self-supported and flexible anode material for LIBs. Benefiting from its 3D interconnected conducting networks, TaS_3 NWs displays excellent electrochemical performance including little capacity fading over 100 cycles (~400 mAh g^{-1} at 0.1 *C* after 100 cycles) and good rate capability (~60 mAh g^{-1} at 10 *C*). The mechanism of lithium-ion insertion/extraction in the TaS_3 NWs was also explored by an ex situ X-ray diffraction method. The excellent performance of TaS_3 NWs results from the 3D interconnected nanowires forming conductive network and facilitating electron transport.[23−25]

Figure 1A, B show the digital photographs of one piece of TaS_3 NWs film. As shown in Figure 1A, the obtained TaS_3 NWs film was cut into small pieces (~0.5 mg, ~0.65 × 0.4 × 0.1 cm), then directly used as self-supported working electrodes for LIBs. The TaS_3 NWs film composed of interconnected nanofibers exhibited high flexibility (Figure 1B). The scanning electron microscopy (SEM) images (Figure 1C) reveals that TaS_3 NW film consists entirely of uniform nanowires without impurity particles or aggregates. The diameter of nanowire is about 120−210 nm (inset of Figure 1C). The continuous and interconnected structure can facilitate both electron and Li-ion transport[26] and electrolyte access to TaS_3.[8] Transmission electron microscopy (TEM) (Figure 1D) was utilized to investigate the microstructure of TaS_3 nanofibers. The obtained TaS_3 nanofibers show uniform structure without obvious crack and fracture, which would guarantee structure stability during cycling. The high resolution (HR) TEM image, shown in the inset of Figure 1D, reveals that the TaS_3 NWs are crystalline with a sandwichlike structure.

Received: February 2, 2015
Accepted: March 3, 2015
Published: March 3, 2015

DOI: 10.1021/acsami.5b00467
ACS Appl. Mater. Interfaces 2015, 7, 5629−5633

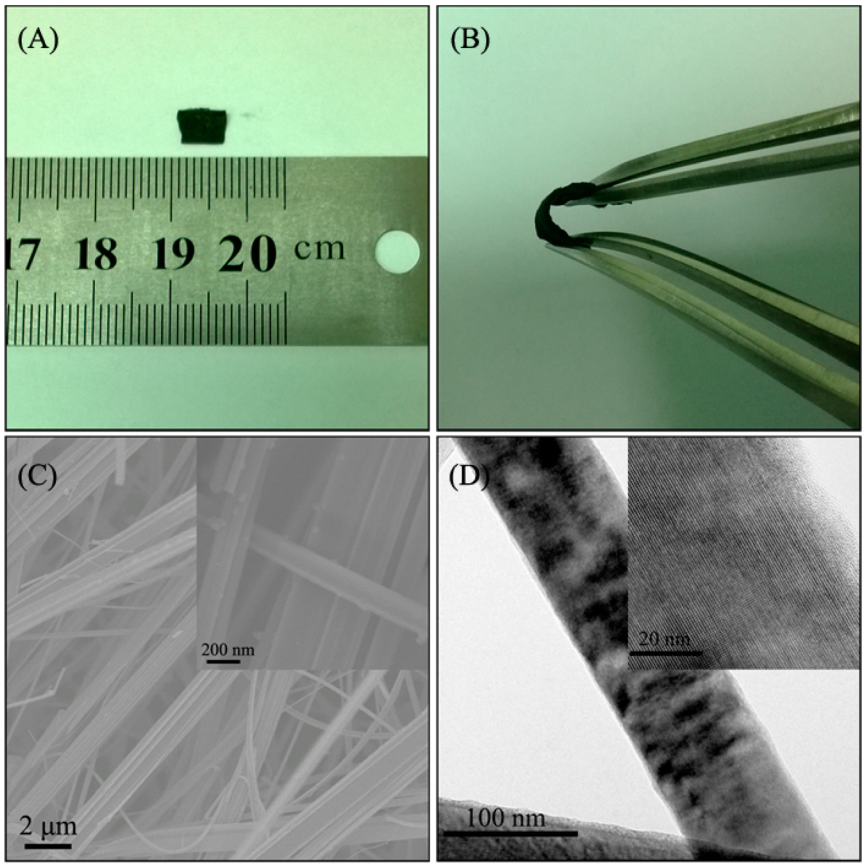

Figure 1. (A, B) Photograph of the free-standing flexible TaS_3 nanowires electrodes (~0.65 × 0.4 × 0.1 cm^3). TaS_3 nanowires show excellent flexibility, bent by two tweezers. (C) Scanning electron microscopy (SEM) images and (D) transmission electron microscopy (TEM) images of TaS_3 nanowires. The inset pictures are corresponding high-magnification images.

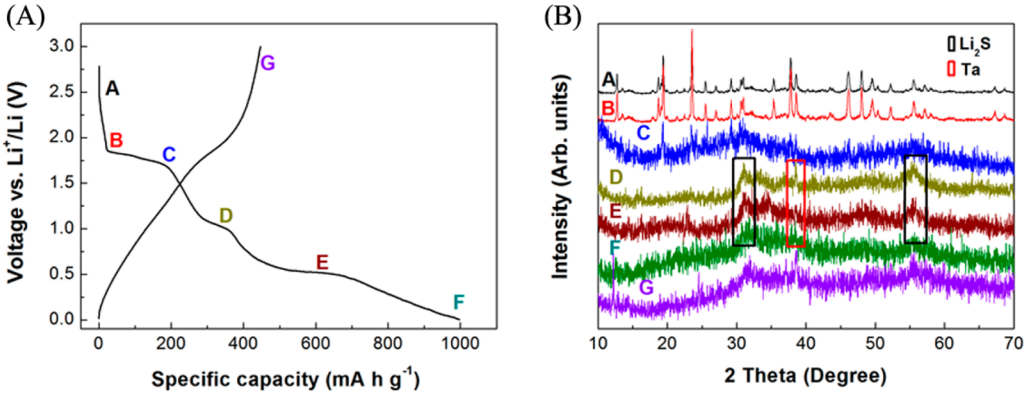

Figure 2. (A) Discharge/charge profiles of TaS_3 nanowires electrode for the first cycle. The voltage stages for such cells were taken, where the letters A−G denote the states of various lithiated electrode materials for corresponding ex situ X-ray diffraction patterns. (B) E situ X-ray diffraction patterns collected at various states of discharge and charge states of TaS_3/Li electrochemical cells.

To investigate the lithium-storage mechanism of TaS_3, we carried out an ex situ X-ray diffraction (XRD) analysis combined with electrochemical measurement. Figure 2A shows the first discharge/charge cycle curve of TaS_3 NWs, with a series of partially lithiated cells at different voltage states denoted as the letters A−G for the ex situ XRD measurement. During the first discharge process, there is no obvious change of XRD patterns when discharged from state A to B, indicating no structural change. After the plateau from state B to C at ~1.75 V, the main peaks of state C correspond to the main peaks of TaS_3 with intensity weakening. This plateau might come from lithium-ion irreversible insertion into atomic layers of TaS_3 as shown in the HRTEM images (Figure 1D) with irreversible capacity. Afterward, TaS_3 would start a reaction to form Li_2S and Ta, associating with electrolyte decomposition at ~0.7 V to form solid-electrolyte-interphase (SEI).[27] During the charge process, Li_2S and Ta would react to form TaS_3, as the XRD pattern of state G suggested. However, the crystallinity of TaS_3 was degraded after the first cycle compared with the original TaS_3 NWs. The mechanism of lithium-ion reaction with TaS_3 can be summarized as $6Li + TaS_3 \leftrightarrow 3Li_2S + Ta$ with an irreversible lithium-ion insertion into atomic layers during the

DOI: 10.1021/acsami.5b00467
ACS Appl. Mater. Interfaces 2015, 7, 5629−5633

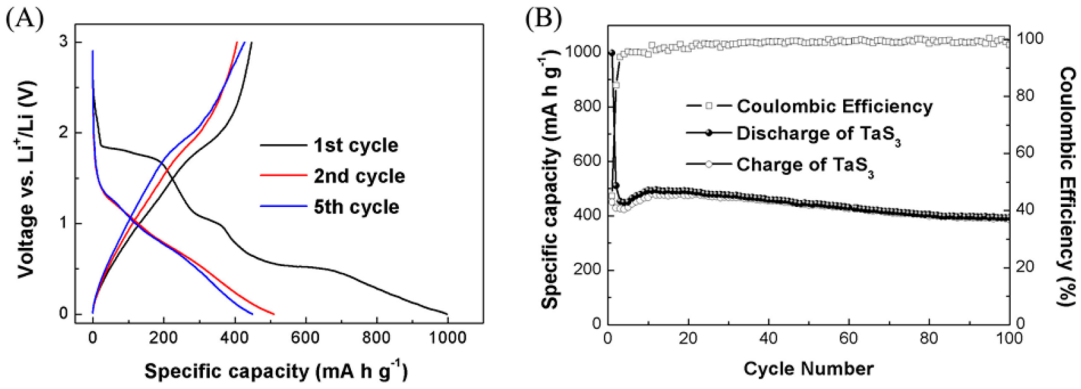

Figure 3. (A) Voltage profiles of TaS_3 nanowires electrode cycled between 0.001 and 3 V vs Li^+/Li at a cycling rate of 0.1C. (B) Electrochemical performance of TaS_3 nanowires electrode cycled between 0.001 and 3 V vs Li^+/Li. Capacity and Colombic efficiency−cycle number curves of TaS_3 nanowires electrode at a cycling rate of 0.1C.

first cycle. The theoretical capacity of TaS_3 is 579 $mAhg^{-1}$ calculated on the basis of this mechanism.

Figure 3A displays the voltage profiles TaS_3 NWs in the voltage window between 0.001−3.0 V (vs Li^+/Li) at a rate of 0.1C. During the first cycle, the discharge and charge step delivers a specific capacity of 997 and 450 mAh g^{-1} for TaS3 NWs, respectively, giving an initial Coulombic efficiency (CE) of ∼45%.The first charge capacity is lower than that of the theoretical capacity, which might attribute to electrolyte decomposition and formation of gel-like polymeric layer (SEI).

Figure 3B shows the capacity retention of TaS_3 NWs at 0.1C. A high reversible specific capacity of about 400 mAh g^{-1} was obtained after 100 cycles, higher than that of commercial graphite materials (372 mAh g^{-1}). After the capacity loss of first cycle, the CE reaches ∼95% after several cycles, indicating the structural stability after the first cycle. Compared with the first lithiation capacity, the capacity decay in Figure 3B was very slow, at only 0.1% decay per cycle. To demonstrate the electrochemical performance of TaS_3 NWs electrode at higher densities, we investigated the rate capability TaS_3 NWs at different cycling current as shown in Figure 4. The TaS_3 NWs

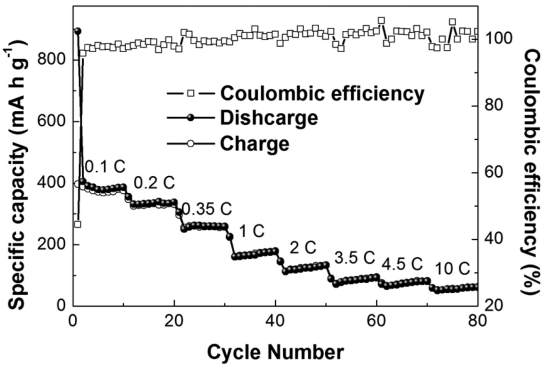

Figure 4. Rate performance and Coulombic efficiency−cycle number curves of TaS_3 nanowires electrodes as a function of discharge rate (0.1−10C).

electrode delivers a rate capacity as high as 340, 260, 180, 130, 90, and 80 mAh g^{-1} when cycled at a current density of 0.2, 0.35, 1, 2, 3.5, and 4.5C, respectively. It could maintain a reversible capacity of 60 mAh g^{-1} even cycled at a current density as high as 10C for 10 cycles, demonstrating excellent rate performance of this free-standing and flexible TaS_3 NWs electrode.

The good cyclability at 0.1C and rate capability of TaS_3 NWs might result from the special self-supported continuous and interconnected structure, which would form a continuous electronic path for fast electron transfer and provide large surface area access to electrolyte and high mechanical flexibility.[8,28] Moreover, the ionic diffusion length would be greatly shortened with the thin film electrode.[29] The integration of all these advantages leads to the potential of the TaS_3 NWs as flexible anode materials for LIBs.

The morphology of the TaS_3 NW electrode was investigated after 100 cycles at a rate of 0.1C to confirm the structure stability of this electrode. As shown in Figure 5, no obvious

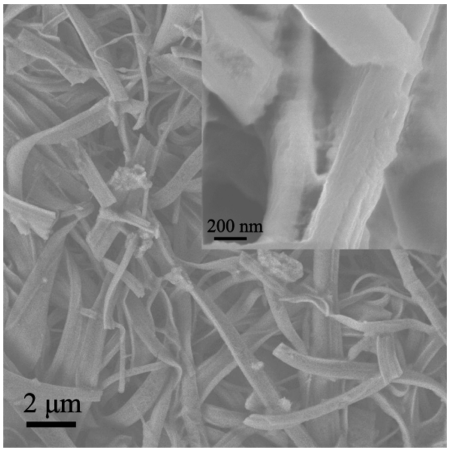

Figure 5. SEM micrographs of TaS_3 nanowires after 100 cycles between 0.001 and 3 V vs Li^+/Li at a cycling rate of 0.1C, inset shows the corresponding high magnification image.

pulverization and fracture appears. The continuous and interconnected structure of TaS_3 NWs remained almost unchanged after 100 cycles. This result indicates that the interconnect NWs network could mitigate the strains caused by the lithium-ion insertion/extraction during cycling and maintain the continuous and interconnected structure to provide a short electron and ion transfer path. Notably, the formation of SEI and some residual electrolyte resulted in a rough surface of TaS_3 NWs.

DOI: 10.1021/acsami.5b00467
ACS Appl. Mater. Interfaces 2015, 7, 5629−5633

To show the potential of application of the flexible anode materials, we further assembled a flexible full battery. Figure 6A

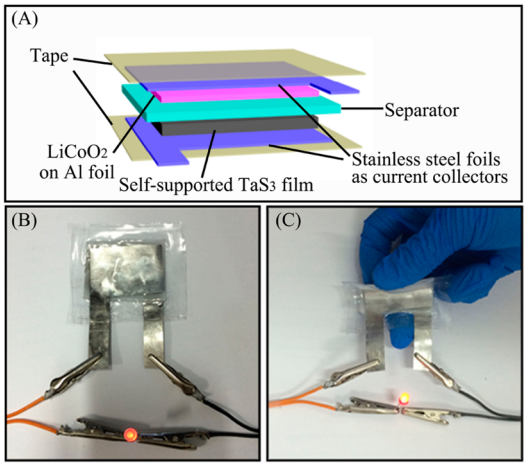

Figure 6. (A) Schematic illustration of a flexible lithium-ion battery assembled using TaS_3 NWs film as the anode and commercial $LiCoO_2$ loaded on Al foil as the cathode; (B–C) digital photographs of a red LED lightened by the flexible battery under (B) flat and (C) bent states.

displays the structure of the prepared flexible full battery, consisting of freestanding TaS_3 NWs film as the anode, a separator, a commercial $LiCoO_2$/Al foil as the cathode and $LiPF_6$-based electrolyte. As shown in Figure 6B, C, the final packaged flexible Li-ion battery is thin and bendable, which could be fully charged to 3 V and is able to light a lighting emitting diode (LED) as the battery is flat and bended, indicating good flexibility of this anode material during cycling.

In summary, we have successfully prepared TaS_3 NWs by a solid state reaction process as a new self-supported and flexible anode material for LIBs. The obtained self-supported and binder free TaS_3 NWs electrodes show good cyclability and rate capability without any protection and conductive layer or additive. It delivers a good reversible capacity of ~400 mAh g^{-1} after 100 cycles at 0.1C with only 0.1% decay per cycle compared with of the initial charge capacity. When cycled at 10C, it still displays a capacity as high as 60 mAh g^{-1}. Moreover, this direct utilization of TaS_3 NWs as novel self-supported and binder-free working electrodes can improve the overall performance of full-cell and simplify the packing process of batteries. This design of nanowires directly used as self-supported and flexible electrodes provides a potential solution to design new flexible electrodes for LIBs or other energy storage systems.

■ ASSOCIATED CONTENT

Supporting Information

Experimental section and additional figures. This material is available free of charge via the Internet at http://pubs.acs.org.

■ AUTHOR INFORMATION

Corresponding Authors

*E-mail: yanyumse@ustc.edu.cn. Tel: +86 551 63607179.
*E-mail: binxiang@ustc.edu.cn.

Notes

The authors declare no competing financial interest.

■ ACKNOWLEDGMENTS

This work was financially supported by the National Natural Science Foundation of China (21171015, 21373195, and 21373196), the "Recruitment Program of Global Experts", the program for New Century Excellent Talents in University (NCET-12-0515), the Fundamental Research Funds for the Central Universities (WK2060140014, WK2060140016), the Collaborative Innovation Center of Suzhou Nano Science and Technology.

■ REFERENCES

(1) Poizot, P.; Laruelle, S.; Grugeon, S.; Dupont, L.; Tarascon, J. M. Nano-Sized Transition-Metal Oxides as Negative-Electrode Materials for Lithium-Ion Batteries. *Nature* **2000**, *407* (6803), 496–499.
(2) Etacheri, V.; Marom, R.; Elazari, R.; Salitra, G.; Aurbach, D. Challenges in the Development of Advanced Li-Ion Batteries: A Review. *Energy Environ. Sci.* **2011**, *4* (9), 3243–3262.
(3) Zhou, G.; Li, F.; Cheng, H. M. Progress in Flexible Lithium Batteries and Future Prospects. *Energy Environ. Sci.* **2014**, *7* (4), 1307–1338.
(4) Gwon, H.; Hong, J.; Kim, H.; Seo, D. H.; Jeon, S.; Kang, K. Recent Progress on Flexible Lithium Rechargeable Batteries. *Energy Environ. Sci.* **2014**, *7* (2), 538–551.
(5) Chew, S. Y.; Ng, S. H.; Wang, J.; Novák, P.; Krumeich, F.; Chou, S. L.; Chen, J.; Liu, H. K. Flexible Free-Standing Carbon Nanotube Films for Model Lithium-Ion Batteries. *Carbon* **2009**, *47* (13), 2976–2983.
(6) Li, X.; Yang, J.; Hu, Y.; Wang, J.; Li, Y.; Cai, M.; Li, R.; Sun, X. Novel Approach toward a Binder-Free and Current Collector-Free Anode Configuration: Highly Flexible Nanoporous Carbon Nanotube Electrodes with Strong Mechanical Strength Harvesting Improved Lithium Storage. *J. Mater. Chem.* **2012**, *22* (36), 18847–18853.
(7) Yue, L.; Zhong, H.; Zhang, L. Enhanced Reversible Lithium Storage in a Nano-Si/Mwcnt Free-Standing Paper Electrode Prepared by a Simple Filtration and Post Sintering Process. *Electrochim. Acta* **2012**, *76*, 326–332.
(8) Li, W.; Yang, Z.; Cheng, J.; Zhong, X.; Gu, L.; Yu, Y. Germanium Nanoparticles Encapsulated in Flexible Carbon Nanofibers as Self-Supported Electrodes for High Performance Lithium-Ion Batteries. *Nanoscale* **2014**, *6* (9), 4532–4537.
(9) Jia, X.; Chen, Z.; Suwarnasarn, A.; Rice, L.; Wang, X.; Sohn, H.; Zhang, Q.; Wu, B. M.; Wei, F.; Lu, Y. High-Performance Flexible Lithium-Ion Electrodes Based on Robust Network Architecture. *Energy Environ. Sci.* **2012**, *5* (5), 6845–6849.
(10) Chen, Z.; To, J. W. F.; Wang, C.; Lu, Z.; Liu, N.; Chortos, A.; Pan, L.; Wei, F.; Cui, Y.; Bao, Z. A Three-Dimensionally Interconnected Carbon Nanotube–Conducting Polymer Hydrogel Network for High-Performance Flexible Battery Electrodes. *Adv. Energy Mater.* **2014**, *4* (12), 1400207 DOI: 10.1002/aenm.201400207.
(11) Huang, X.; Sun, B.; Chen, S.; Wang, G. Self-Assembling Synthesis of Free-Standing Nanoporous Graphene–Transition-Metal Oxide Flexible Electrodes for High-Performance Lithium-Ion Batteries and Supercapacitors. *Chem.—Asian J.* **2014**, *9* (1), 206–211.
(12) Zhao, Y.; Li, X.; Yan, B.; Li, D.; Lawes, S.; Sun, X. Significant Impact of 2d Graphene Nanosheets on Large Volume Change Tin-Based Anodes in Lithium-Ion Batteries: A Review. *J. Power Sources* **2015**, *274*, 869–884.
(13) Hu, Y.; Sun, X. Flexible Rechargeable Lithium Ion Batteries: Advances and Challenges in Materials and Process Technologies. *J. Mater. Chem. A* **2014**, *2* (28), 10712–10738.
(14) Li, X.; Wang, C. Engineering Nanostructured Anodes Via Electrostatic Spray Deposition for High Performance Lithium Ion Battery Application. *J. Mater. Chem. A* **2013**, *1* (2), 165–182.
(15) Zhang, N.; Yi, R.; Wang, Z.; Shi, R.; Wang, H.; Qiu, G.; Liu, X. Hydrothermal Synthesis and Electrochemical Properties of Alpha-Manganese Sulfide Submicrocrystals as an Attractive Electrode

DOI: 10.1021/acsami.5b00467
ACS Appl. Mater. Interfaces 2015, 7, 5629–5633

Material for Lithium-Ion Batteries. *Mater. Chem. Phys.* **2008**, *111* (1), 13−16.
(16) Li, L.; Cabán-Acevedo, M.; Girard, S. N.; Jin, S. High-Purity Iron Pyrite (Fes2) Nanowires as High-Capacity Nanostructured Cathodes for Lithium-Ion Batteries. *Nanoscale* **2014**, *6* (4), 2112−2118.
(17) Yan, J. M.; Huang, H. Z.; Zhang, J.; Liu, Z. J.; Yang, Y. A Study of Novel Anode Material Cos2 for Lithium Ion Battery. *J. Power Sources* **2005**, *146* (1−2), 264−269.
(18) Nishio, Y.; Kitaura, H.; Hayashi, A.; Tatsumisago, M. All-Solid-State Lithium Secondary Batteries Using Nanocomposites of Nis Electrode/Li2s-P2s5 Electrolyte Prepared Via Mechanochemical Reaction. *J. Power Sources* **2009**, *189* (1), 629−632.
(19) Wang, Q.; Li, J. Facilitated Lithium Storage in Mos2 Overlayers Supported on Coaxial Carbon Nanotubes. *J. Phys. Chem. C* **2007**, *111* (4), 1675−1682.
(20) Wang, G. X.; Bewlay, S.; Yao, J.; Liu, H. K.; Dou, S. X. Tungsten Disulfide Nanotubes for Lithium Storage. *Electrochem. Solid-State Lett.* **2004**, *7* (10), A321−A323.
(21) Chen, G. Y.; Wei, Z. Y.; Jin, B.; Zhong, X. B.; Wang, H.; Zhang, W. X.; Liang, J. C.; Jiang, Q. Hydrothermal Synthesis of Copper Sulfide with Novel Hierarchical Structures and Its Application in Lithium-Ion Batteries. *Appl. Surf. Sci.* **2013**, *277*, 268−271.
(22) Golovnya, A. V.; Pokrovskii, V. Y.; Shadrin, P. M., Coupling of the Lattice and Superlattice Deformations and Hysteresis in Thermal Expansion for the Quasi-One-Dimensional Conductor Tas3. *Phys. Rev. Lett.* **2002**, *88* (24).
(23) Zhu, C.; Mu, X.; Vanaken, P. A.; Yu, Y.; Maier, J. Single-Layered Ultrasmall Nanoplates of Mos2 Embedded in Carbon Nanofibers with Excellent Electrochemical Performance for Lithium and Sodium Storage. *Angew. Chem., Int. Ed.* **2014**, *53* (8), 2152−2156.
(24) Liu, J.; Tang, K.; Song, K.; Van Aken, P. A.; Yu, Y.; Maier, J. Tiny Li4ti5o12 Nanoparticles Embedded in Carbon Nanofibers as High-Capacity and Long-Life Anode Materials for Both Li-Ion and Na-Ion Batteries. *Phys. Chem. Chem. Phys.* **2013**, *15* (48), 20813−20818.
(25) Zhu, C. B.; Yu, Y.; Gu, L.; Weichert, K.; Maier, J. Electrospinning of Highly Electroactive Carbon-Coated Single-Crystalline Lifepo4 Nanowires. *Angew. Chem., Int. Ed.* **2011**, *50* (28), 6278−6282.
(26) Ko, Y. D.; Kang, J. G.; Lee, G. H.; Park, J. G.; Park, K. S.; Jin, Y. H.; Kim, D. W. Sn-Induced Low-Temperature Growth of Ge Nanowire Electrodes with a Large Lithium Storage Capacity. *Nanoscale* **2011**, *3* (8), 3371−3375.
(27) Liu, H.; Wang, G.; Liu, J.; Qiao, S.; Ahn, H. Highly Ordered Mesoporous Nio Anode Material for Lithium Ion Batteries with an Excellent Electrochemical Performance. *J. Mater. Chem.* **2011**, *21* (9), 3046−3052.
(28) Jiang, J.; Li, Y.; Liu, J.; Huang, X.; Yuan, C.; Lou, X. W. Recent Advances in Metal Oxide-Based Electrode Architecture Design for Electrochemical Energy Storage. *Adv. Mater.* **2012**, *24* (38), 5166−5180.
(29) Liu, J.; Song, K.; Van Aken, P. A.; Maier, J.; Yu, Y. Self-Supported Li4ti5o12-C Nanotube Arrays as High-Rate and Long-Life Anode Materials for Flexible Li-Ion Batteries. *Nano Lett.* **2014**, *14* (5), 2597−2603.

DOI: 10.1021/acsami.5b00467
ACS Appl. Mater. Interfaces 2015, 7, 5629−5633